





Article

Jeankempite, $\text{Ca}_5(\text{AsO}_4)_2(\text{AsO}_3\text{OH})_2(\text{H}_2\text{O})_7$, a new arsenate mineral from the Mohawk Mine, Keweenaw County, Michigan, USA

Travis A. Olds^{1*} , Anthony R. Kampf², Fabrice Dal Bo³, Peter C. Burns^{3,4}, Xiaofeng Guo⁵ and John S. McCloy^{5,6} 

¹Section of Minerals and Earth Sciences, Carnegie Museum of Natural History, 4400 Forbes Avenue, Pittsburgh, Pennsylvania 15213, USA; ²Mineral Sciences Department, Natural History Museum of Los Angeles County, 900 Exposition Boulevard, Los Angeles, CA 90007, USA; ³Department of Civil and Environmental Engineering and Earth Sciences, University of Notre Dame, Notre Dame, IN 46556, USA; ⁴Department of Chemistry and Biochemistry, University of Notre Dame, Notre Dame, IN 46556, USA; ⁵Department of Chemistry, Washington State University, Pullman, WA 99163, USA; and ⁶School of Mechanical and Materials Engineering, Washington State University, Pullman, WA, 99163, USA

Abstract

Jeankempite, $\text{Ca}_5(\text{AsO}_4)_2(\text{AsO}_3\text{OH})_2(\text{H}_2\text{O})_7$, is a new mineral species (IMA2018-090) discovered amongst coatings of arsenate minerals on oxidised copper arsenides from the Mohawk No. 2 mine, Mohawk, Keweenaw County, Michigan, USA. The new mineral occurs as lamellar bundles of colourless to white plates up to 1 mm wide and is visually indistinguishable from guérinite, with which it forms intergrowths. Jeankempite is transparent to translucent with a waxy lustre and white streak, is non-fluorescent under longwave and shortwave ultraviolet illumination, has a Mohs hardness of ~ 1.5 and brittle tenacity with uneven fracture. Crystals are flattened on $\{01\bar{1}\}$ and exhibit perfect cleavage on $\{01\bar{1}\}$. Optically, jeankempite is biaxial (+), $\alpha = 1.601(2)$, $\beta = 1.607(2)$, $\gamma = 1.619(2)$ (white light); $2V_{\text{meas.}} = 72(2)^\circ$ and $2V_{\text{calc.}} = 71.0^\circ$. The empirical formula is $(\text{Ca}_{4.97}\text{Na}_{0.013}\text{Mg}_{0.017})(\text{As}_{3.99}\text{Sb}_{0.01})_4\text{O}_{23}\text{H}_{16}$, based on 23 O and 16 H atoms per formula unit. Thermogravimetric analysis indicates that jeankempite undergoes four weight losses totalling 16.82%, close to the expected loss of 16.30%, corresponding to eight H_2O . Jeankempite is triclinic, $P\bar{1}$, $a = 6.710(6)$, $b = 14.901(14)$, $c = 15.940(15)$ Å, $\alpha = 73.583(12)^\circ$, $\beta = 81.984(12)^\circ$, $\gamma = 82.754(12)^\circ$, $V = 1507(2)$ Å³ and $Z = 3$. The final structure was refined to $R_1 = 0.0591$ for 2781 reflections with $I_{\text{obs}} > 3\sigma I$. The crystal structure of jeankempite is built from a network of edge- and vertex-sharing CaO_6 , CaO_7 and AsO_4 polyhedra, and we hypothesise that the new mineral has formed due to a topotactic reaction brought on by dehydration of preexisting guérinite.

Keywords: Jeankempite, new mineral, arsenate, guérinite, topotactic reaction, crystal structure, Mohawk mine, Michigan, USA

(Received 1 September 2020; accepted 19 November 2020; Accepted Manuscript published online: 25 November 2020; Associate Editor: Michael Rumsey)

Introduction

Natural processes such as volcanism, forest fires, biological activity and weathering of arsenic-bearing minerals are collectively responsible for the release of most arsenic into the environment; however, human activities have led to highly concentrated arsenic contamination (Smedley and Kinniburgh, 2002; Han *et al.*, 2003; Majzlan *et al.*, 2014). Fossil fuel combustion, metal smelting and the use of arsenic-based agricultural products and wood preservatives are just some of the dominant human-generated pollution sources of arsenic (WHO, 2001). Within the last decade, large accumulations of electronic waste (e-waste) and extensive efforts to recycle them have also become major sources of arsenic pollution (Asante *et al.*, 2012; Amphalop *et al.*, 2020), though by a significant margin, the highest concentrations of arsenic contamination are found in the environment near mining and smelting operations (Smedley and Kinniburgh, 2002). Post-mining oxidation of arsenic-bearing ore and slags can lead to the formation

of secondary arsenate minerals, and over 400 species are currently known. The most prolific occurrence of arsenic minerals is found in the Lavrion Mining District, Greece, which hosts numerous mines and slag heaps that collectively are the type locality for 10 minerals containing various arsenic oxyanions (AsO_3^{3-} , AsO_4^{3-} , $\text{AsO}_3\text{OH}^{2-}$, $\text{As}_2\text{O}_5^{4-}$) and that host over 160 additional As-bearing species (<https://www.mindat.org>; accessed August 2020).

Arsenic speciation in oxic groundwater is dominantly As^{5+} , occurring as the dihydrogen arsenate anion, $\text{AsO}_2(\text{OH})_2^{1-}$, between pH ~ 2 and 7, and as the hydrogen arsenate anion, $\text{AsO}_3\text{OH}^{2-}$, between pH ~ 7 and 12 (Cullen and Reimer, 1989). Due to its high toxicity especially in the As^{3+} oxidation state, mobility and prevalence as a pollutant, it is crucial to understand the crystal chemistry and stability of As-bearing minerals. Here we describe the crystal structure, along with the spectroscopic and thermogravimetric properties of the new arsenate mineral jeankempite, which contains the hydrogen arsenate anion, $\text{AsO}_3\text{OH}^{2-}$.

The name jeankempite honours Jean Petermann Kemp Zimmer (1917–2001), curator of the A. E. Seaman Mineral Museum in Houghton, MI, USA, from 1975 to 1986. She received a B.S. in Geology from the Michigan College of Mining and Technology (MCMT), which is now Michigan Technological University (MTU), graduating with honours in 1939. In that

*Author for correspondence: Travis A. Olds, Email: oldst@carnegiemnh.org

Cite this article: Olds T.A., Kampf A.R., Dal Bo F., Burns P.C., Guo X. and McCloy J.S. (2020) Jeankempite, $\text{Ca}_5(\text{AsO}_4)_2(\text{AsO}_3\text{OH})_2(\text{H}_2\text{O})_7$, a new arsenate mineral from the Mohawk Mine, Keweenaw County, Michigan, USA. *Mineralogical Magazine* 84, 959–969. <https://doi.org/10.1180/mgm.2020.92>

same year, Jean was awarded the Geology Key, which was the highest departmental academic award at the time. She obtained a Master's Degree in Geology from the University of Michigan in 1940 and subsequently taught mineralogy in the MCMT Geology Department until 1943. From 1967 to 1975, Jean served as Assistant Curator to Kiril Spiroff, afterwards succeeding him as Curator until 1986. Jean designed the display cases and developed the cataloguing system still in use at the Seaman Museum today, and in 2002, she was posthumously awarded the Charles A. Salotti Earth Science Education Award by the Seaman Mineral Museum Society (Dyl, 2002).

The mineral and its name were approved by the Commission on New Minerals, Nomenclature and Classification of the International Mineralogical Association (IMA2018-090, Olds *et al.*, 2018). The holotype specimen is deposited in the collection of the A.E. Seaman Mineral Museum with catalogue number DM 31705. Crystals from the holotype specimen are deposited in the Natural History Museum of Los Angeles County, under catalogue number 66799.

Occurrence

Jeankempite was discovered amongst coatings of arsenate minerals on a specimen of oxidised copper arsenides in calcite from the Mohawk No. 2 mine, Mohawk, Keweenaw County, Michigan, USA (47°17'40"N, 88°22'35"W). The Mohawk mine is located adjacent to and underneath the village of Mohawk, ~14 miles north-northeast of Houghton, Michigan, and is well-known to mineral collectors for the occurrence of 'mohawkite', a mixture of copper and nickel arsenides consisting primarily of domeykite (Cu_3As), algodonite ($\text{Cu}_{6\pm x}\text{As}$) and arsenical copper with rammelsbergite (NiAs_2) and rare domeykite- β (Cu_{3-x}As) (Moore, 1962). Considering the semi-metallic nature of As, the term 'copper arsenide' may not be correctly applied to certain Cu-As minerals, especially species with large ratios of Cu:As that contain primarily intermetallic Cu-Cu bonds, such as algodonite. Currently, the International Union of Pure and Applied Chemistry (IUPAC, 2005) provides no guidance for the naming of intermetallic compounds and we prefer to retain historical use of the term 'copper arsenide', acknowledging that this nomenclature is subject to change.

The arsenide-bearing fissure at the Mohawk mine was exposed by a large stope that spanned the 11th and 12th levels, where the arsenide veins varied in thickness, reaching up to four feet wide in places. We have been unable to trace by whom or when the holotype sample was collected; however, Moore (1971) explains that the actions of mine water on the arsenides led to the formation of "numerous hydrated calcium and copper arsenates", suggesting it may be at least 60 years old, if brought to the surface by Moore (or others) before the shaft was sealed in the mid 1960s.

Copper and nickel arsenides occurred in great abundance at the Mohawk mine, with over 230,000 pounds removed between 1900 and 1901; arsenides also occurred as large lens-shaped masses in fissures intersecting bedded copper deposits at the nearby and interconnected Ahmeek and Seneca mines, and several large fissures were encountered sporadically in the Isle Royale lode further north (Butler and Burbank, 1929; Robinson, 2004). In fact, native copper was noted to be arsenical throughout the Keweenaw copper district. Deep lodes positioned near the intersection of the Keweenaw fault generally contained higher arsenic content than those exploited nearer to the surface and it has been suggested by Butler and Burbank (1929, p. 115) that,



Fig. 1. Lamellar bundles of jeankempite intergrown with guérinite on altered α -domeykite, with annabergite, calcite and cream coloured ankerite. Horizontal field of view is 3.0 mm.

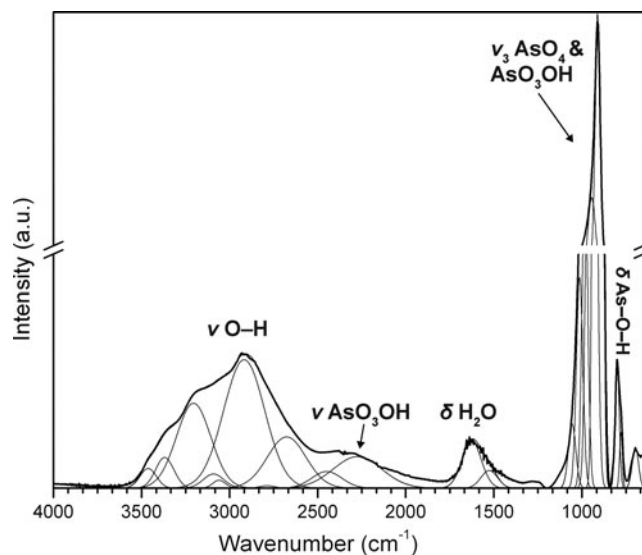


Fig. 2. The infrared spectrum of jeankempite from 4000 to 650 cm^{-1} .

"...this may be so because the solution that mineralized these lodes had flowed for a relatively short distance in them and therefore had been less completely oxidized than the solution that mineralized the higher lodes". The hypothesis remains untested, though, to some extent, is supported in that arsenide veins and arsenical copper were commonly encountered near large fissures that may have allowed an As-bearing solution to ascend without experiencing strong volatilisation or oxidation. Further details on the geology of the Keweenaw, including the age and the prevailing model of copper deposition can be found in Bornhorst *et al.* (1988) and Brown (2006), respectively.

Jeankempite occurs intimately with calcite, ankerite and several copper arsenides, along with other arsenates such as guérinite, $\text{Ca}_5(\text{AsO}_4)_2(\text{AsO}_3\text{OH})_2(\text{H}_2\text{O})_9$, rauenthalite, $\text{Ca}_3(\text{AsO}_4)_2(\text{H}_2\text{O})_{10}$, annabergite, $\text{Ni}_3(\text{AsO}_4)_2(\text{H}_2\text{O})_8$, lavendulan,

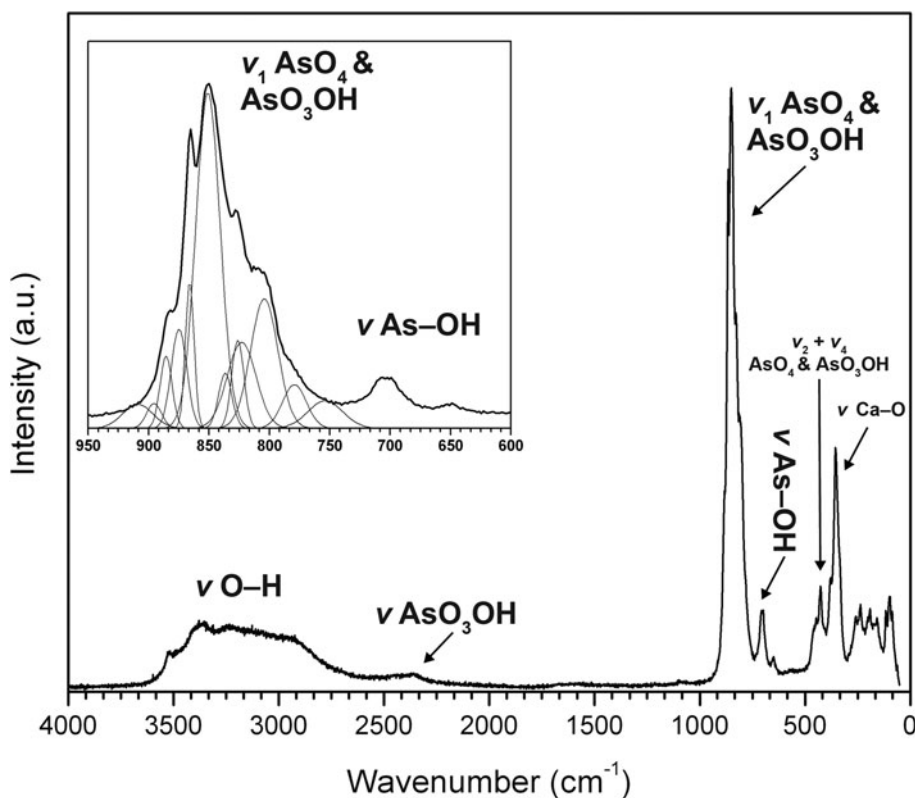


Fig. 3. The Raman spectrum of jeankempite from 4000 to 50 cm^{-1} .

$\text{NaCaCu}_5(\text{AsO}_4)_4\text{Cl}(\text{H}_2\text{O})_5$ and an additional unidentified calcium arsenate hydrate phase detected during powder X-ray diffraction analyses. Sponge-like, brown to yellow-brown blebs of an unidentified copper arsenide mineral are also found on the surfaces of oxidised specimens. The arsenates in this assemblage formed due to post-mining oxidation of copper and nickel arsenides, accompanied by dissolution of calcite as a source of calcium. Jeankempite, which we hypothesise has formed by dehydration of guérinite, possesses a distinct structure that fills gaps in our knowledge of the structural relationships between the hydrated calcium arsenate minerals. Although the dehydration of guérinite to jeankempite was not directly observed, it may occur *via* a topotactic transition that was necessarily slow to yield the relatively large and well-crystallised domains studied here.

Physical and optical properties

Jeankempite occurs as lamellar bundles of plates up to 1 mm wide and is visually indistinguishable from guérinite, with which it forms intergrowths (Fig. 1). Jeankempite is transparent to translucent with a waxy lustre and white streak, has a Mohs hardness of *ca.* 1.5 and has brittle tenacity with uneven fracture. No fluorescence was observed under longwave or shortwave ultraviolet illumination. Crystals exhibit perfect cleavage on $\{01\bar{1}\}$ and are flattened on $\{01\bar{1}\}$; no other forms could be distinguished with certainty. The density is $2.92(2) \text{ g}\cdot\text{cm}^{-3}$ measured by flotation in a mixture of diiodomethane and toluene; the calculated density is $2.93 \text{ g}\cdot\text{cm}^{-3}$ based on the empirical formula and $2.92 \text{ g}\cdot\text{cm}^{-3}$ based on the ideal formula.

Optically, jeankempite is biaxial (+), with $\alpha = 1.601(2)$, $\beta = 1.607(2)$ and $\gamma = 1.619(2)$, measured in white light. The $2V_{\text{meas.}} =$

$72(2)^\circ$ based on extinction data collected on a spindle stage and analysed using *EXCALIBUR* (Gunter *et al.*, 2004); the $2V_{\text{calc.}} = 71.0^\circ$. Dispersion is weak, $r < v$. Pleochroism is absent and the optical orientation is $X \wedge c = 45^\circ$, $Y \wedge b = 35^\circ$ and $Z \wedge a = 27^\circ$. The Gladstone–Dale compatibility, $1 - (K_p/K_c)$, is -0.010 (superior) for the ideal formula and -0.017 (superior) for the empirical formula using the k values given by Mandarino (2007).

Infrared spectroscopy

The attenuated total reflectance (ATR) Fourier-transform infrared (FTIR) spectrum was collected using a SENSIR Technologies IlluminatIR with a liquid N_2 cooled MCT detector mounted to an Olympus BX51 microscope. A “ContactIR” ATR objective (ZnSe and diamond composite lens) was pressed into jeankempite crystals and the spectrum was measured from 4000 to 650 cm^{-1} (Fig. 2). The following IR and Raman band assignments for jeankempite are made with guidance from Makreski *et al.* (2018, 2019). A broad, multicomponent band spanning from ~ 3500 to $\sim 2100 \text{ cm}^{-1}$ is attributed to the ν (O–H) stretching vibrations of water molecules and AsO_3OH units. The series of fitted bands in this region have maxima at 3392, 3170, 2887, 2680 and 2390 cm^{-1} . Approximate O–H...O hydrogen bond-lengths calculated from the observed stretching frequencies occur within the range ~ 2.8 to 2.6 \AA using the correlation given by Libowitzky (1999). A broad band found at 1624 cm^{-1} is assigned to the ν_2 (δ)-bending vibration of water molecules. The weak set of enveloped bands at ~ 1280 and 1242 cm^{-1} probably correspond to δ (O–H) bending vibrations of AsO_3OH units, and the very strong band at 911 cm^{-1} with weak shoulders at 948 and 978 cm^{-1} is attributed to the ν_3 symmetric stretching vibrations of AsO_4 and AsO_3OH units. A second set of weak overlapping bands at

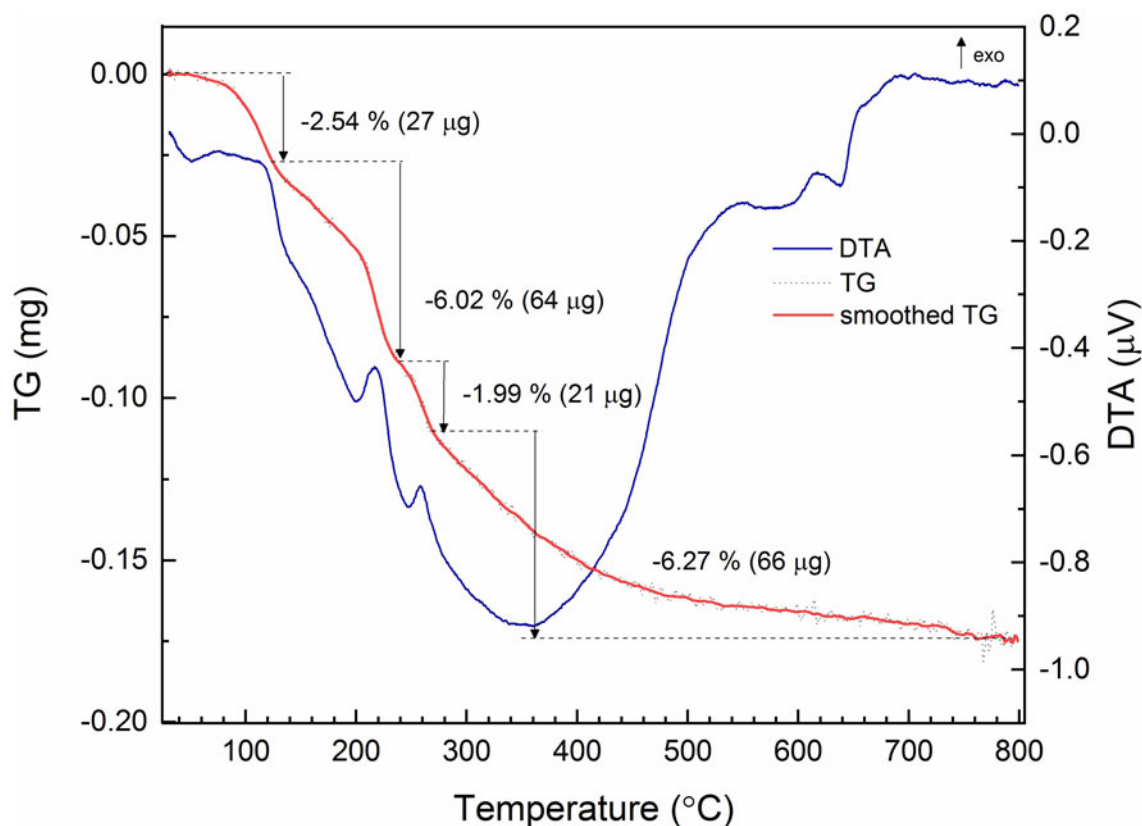


Fig. 4. DSC-TGA analysis of jeankempite. The DSC trace is given as the blue solid line, with the raw TGA trace in black dash and smoothed TGA trace in solid bold red.

799 and 773 cm^{-1} are assigned to either bending δ (As–O–H) or stretching ν_1 (As–O–H/As–O) modes, while the weak and broad band at 689 cm^{-1} is assigned to libration modes of H_2O coinciding with ν (As–OH) modes.

Raman spectroscopy

The Raman spectrum of jeankempite was measured using a Horiba XploRA PLUS instrument with 532 nm diode laser operated at full power, with a spot size of 100 μm and $\sim 5 \text{ cm}^{-1}$ resolution (Fig. 3). The spectrum was acquired using a 100 \times objective, from 5 to 4000 cm^{-1} using 20 exposures of 5 s, aligned roughly perpendicular to the cleavage plane. A set of broad bands related to ν (O–H) stretching vibrations of H_2O molecules and AsO_3OH groups occurs between ~ 3600 and 2700 cm^{-1} with fitted maxima at 3604, 3524, 3487, 3382, 3259, 3182, 3092, 2933 and 2734 cm^{-1} . A single weak band at 2381 cm^{-1} is assigned to ν (O–H) stretching modes of AsO_3OH groups. A very weak band at $\sim 1090 \text{ cm}^{-1}$ originates from δ (O–H) bending modes of AsO_3OH groups. The spectrum between ~ 910 to $\sim 770 \text{ cm}^{-1}$ displays a complex set of overlapping bands due to ν_3 and ν_1 stretching modes of AsO_4 and AsO_3OH groups. This region was successfully fit using 12 bands, in accordance with the expected number of bands from six independent arsenate groups in the structure, which lie at 909, 891, 884, 872, 866, 851, 837, 826, 823, 804, 779 and 770 cm^{-1} . A moderately intense band at 704 cm^{-1} and weak band at 650 cm^{-1} are both assigned to stretching ν (As–OH) modes. The weak set of overlapping bands at 448, 426 and 407 cm^{-1} belong to ν_4 and ν_2 stretching modes of AsO_4 and

Table 1. Analytical data (wt.%) for jeankempite.

Constituent	Mean	Range	S.D.	Theoretical	Standard
As_2O_5	51.54	50.46–52.69	0.79	51.99	Arsenopyrite
SO_3	0.03	0–0.05	0.03	-	Anhydrite
CaO	31.26	30.83–31.87	0.64	31.71	Anhydrite
MgO	0.06	0–0.29	0.10	-	Olivine
Na_2O	0.12	0–0.33	0.12	-	Albite
H_2O^*	16.18	-	-	16.30	
Total	99.19			100.00	

S.D. – standard deviation. *Based on the structure.

AsO_3OH groups. Three overlapping bands of moderate intensity at 379, 354 and 334 cm^{-1} are assigned to Ca–O stretching vibrations, possibly in coincidence with ν_2 (AsO_3OH) stretches. Remaining fitted bands with moderate to low intensity at 260, 250, 238, 195, 177, 157, 115, 98 and 87 cm^{-1} originate from lattice vibrations.

DSC-TGA measurements

Differential scanning calorimetry (DSC)-thermal gravimetric analysis (TGA) measurements were performed with a Setaram SetSYS Evolution instrument. Powdered crystals (1.056 mg) were placed into an alumina crucible and heated under N_2 flow (20 mL/min) from 30°C to 800°C at 10°C/min. The retrieved material after thermal decomposition was a mixture of CaO (5 mol.) and As_2O_5 (2 mol.). The TG curve (Fig. 4) indicates at least four independent losses occurred in this heating range, totalling 16.82%

Table 2. Powder X-ray data for jeankempite (*d* values in Å).

<i>l</i> _{obs}	<i>l</i> _{calc}	<i>d</i> _{obs}	<i>d</i> _{calc}	<i>hkl</i>
	2		15.1989	0 0 1
100	100	9.25	9.2218	0 1 1
	4		7.6111	0 1 2
80	17, 9, 16	5.39	5.4372, 5.3940, 5.3582	1 1 2, 1 1 1, 1 1 1
	4		5.2794	1 2 1
5	3	4.747	4.7446	0 3 0
24	5, 9, 5	4.613	4.6433, 4.6109, 4.5657	1 1 2, 0 2 2, 1 2 1
	3		4.2527	1 0 3
23	9	4.072	4.0511	0 3 3
	3		4.0341	1 3 0
41	16, 3, 3	3.791	3.8055, 3.7955, 3.7411	0 2 4, 1 2 2, 1 3 3
18	10	3.622	3.6194	0 4 2
18	14	3.554	3.5503	1 2 4
10	7	3.392	3.3887	1 4 2
	4		3.3083	2 0 0
60	30, 12	3.180	3.1886, 3.1579	2 2 1, 1 1 4
24	11, 10	3.092	3.0942, 3.0739	1 2 4, 0 3 3
26	15, 4	2.995	3.0050, 2.9979	1 1 5, 1 4 2
86	11, 30, 10	2.954	2.9649, 2.9456, 2.9197	1 1 4, 0 5 1, 2 0 3
46	5, 9, 13	2.854	2.8665, 2.8567, 2.8380	1 4 1, 2 2 1, 2 3 0
	3		2.7953	1 3 3
20	14	2.701	2.7085	1 1 5
9	3, 5	2.648	2.6580, 2.6413	1 4 5, 2 0 3
28	13, 4	2.605	2.6045, 2.5824	2 3 0, 1 5 1
	2		2.5370	0 3 6
	2		2.5049	1 3 6
	2		2.4570	0 5 2
7	4	2.422	2.4341	1 2 5
	2		2.4010	2 4 1
8	3, 4	2.374	2.3773, 2.3723	2 3 3, 0 6 0
5	3, 2, 2	2.315	2.3394, 2.3217, 2.3008	1 2 5, 2 2 4, 1 6 0
11	5	2.270	2.2840	1 0 6
	2		2.2534	0 2 7
	2		2.2508	2 5 4
15	3, 4	2.1843	2.1871, 2.1819	2 3 6, 1 4 4
	2		2.1723	1 4 4
7	2, 5	2.0915	2.0996, 2.0836	2 6 3, 2 5 1
13	3, 2, 3	2.0286	2.0331, 2.0240, 2.0149	1 6 6, 1 1 7, 2 5 2
8	2, 3	1.9565	1.9567, 1.9405	1 7 5, 1 1 8
18	4, 4	1.9308	1.9320, 1.9262	3 1 5, 3 1 4
22	4, 7	1.8951	1.8923, 1.8905	1 6 3, 2 7 2
27	5, 6	1.8567	1.8664, 1.8530	3 4 5, 1 6 6
	2		1.8383	1 5 7
34	4, 11	1.7995	1.8124, 1.7962	3 3 6, 3 1 4
	2		1.7823	2 1 8
	2		1.7799	1 5 5
13	2	1.7553	1.7535	1 3 9
11	4, 2	1.7127	1.7211, 1.6999	3 2 5, 1 2 8
19	3, 5, 2, 3	1.6798	1.6869, 1.6754, 1.6594, 1.6542	2 7 2, 2 8 1, 2 6 3, 4 0 0
32	3, 2, 3, 3, 2	1.6278	1.6371, 1.6322, 1.6302, 1.6235, 1.6212	0 8 2, 3 6 6, 4 1 1, 3 2 5, 1 8 7
	2		1.6131	4 2 4
20	2, 4, 5	1.5871	1.5943, 1.5837, 1.5753	4 4 2, 3 4 5, 2 0 9
17	2, 2, 2	1.5595	1.5642, 1.5478, 1.5463	4 2 1, 3 3 6, 1 9 3
8	3, 3	1.5291	1.5304, 1.5192	2 8 1, 4 5 1
	2		1.4878	3 6 3,
13	2, 3, 2	1.4745	1.4742, 1.4728, 1.4706	2 5 10, 0 10 2, 0 3 9
6	2	1.4603	1.4609	4 3 3
5	2, 2	1.4419	1.4418, 1.4396	2 0 9, 3 6 3

The strongest lines are given in bold.

(~8.25 H₂O), close to the expected loss for jeankempite, 16.30%, or eight H₂O. Powder diffraction analysis indicated that crystals of jeankempite are associated intimately with guérinite and we expect that the excess loss measured is due to this impurity. We estimate the heated sample contained ~13% guérinite, assuming that this mineral transforms into jeankempite within the first ~120°C; however, there is no evidence that rapid heating of guérinite produces jeankempite. Indeed, the relatively broad and multicomponent

endothermic reaction between ~60 and ~120°C indicates that a complex structural rearrangement has occurred in this temperature range. A 6.02% mass loss between 120–210°C corresponds to the loss of ~three H₂O groups from jeankempite, which occurred in at least two steps as evidenced by two endothermic reactions. The strong endothermic reaction beginning at ~150°C may correspond to the formation of an unidentified tetrahydrate intermediate that is relatively stable, though more experiments are needed to

Table 3. Data collection and structure refinement details for jeankempite.

Crystal data	
Structural formula	Ca ₅ As ₄ O _{22.733}
Crystal size (μm)	60 × 50 × 100
Space group	<i>P</i> $\bar{1}$
Temperature (K)	150(2)
<i>a</i> , <i>b</i> , <i>c</i> (Å)	6.710(6), 14.901(14), 15.940(15)
α , β , γ (°)	73.583(12), 81.984(12), 82.754(12)
<i>V</i> (Å ³)	1507(2)
<i>Z</i>	3
Density (for above formula) (g. cm ⁻³)	2.855
Absorption coefficient (mm ⁻¹)	7.974
Data collection	
Diffractometer	Bruker Quazar II with Apex II detector
X-ray radiation, wavelength (Å)	MoK α , λ = 0.71075
Voltage, current	50 kV, 60 mA
<i>F</i> (000)	1242
θ range (°)	1.34 to 26.83
Reflections collected/unique	16,953/6407; <i>R</i> _{int} = 0.1046
Reflections with <i>I</i> _{obs} > 3 σ (<i>I</i>)	2781
Completeness to θ° _{full}	99%
Index ranges	-8 ≤ <i>h</i> ≤ 8, -18 ≤ <i>k</i> ≤ 18, -20 ≤ <i>l</i> ≤ 20
Refinement	
Refinement method	Full-matrix least-squares on <i>F</i> ²
Parameters refined (restraints)	271 (0)
GoF(obs/all)	1.27/1.27
<i>R</i> _{obs} , <i>wR</i> _{obs}	0.0591, 0.1312
<i>R</i> _{all} , <i>wR</i> _{all}	0.0591, 0.1312
$\Delta\rho_{\max}$, $\Delta\rho_{\min}$ (e ⁻ Å ⁻³)	+1.23/-1.27

state definitively. The weight equivalent to one H₂O group, 1.99%, is lost between 238 and 267°C, possibly due to decomposition of OH from the two hydrogen arsenate groups. This process may begin at lower temperatures, though, as elimination of OH from AsO₃OH units between ~200 and 300°C was observed during hot-stage FTIR studies of pharmacolite and picroparmacolite (Makreski *et al.*, 2019). The final loss from 267 to 800°C probably corresponds to the dehydroxylation of intermediate phases of undetermined stoichiometry (equivalent to ~three H₂O groups) and transformation to the oxides.

Chemical composition

Chemical analyses (*n* = 7) were performed using a JEOL JXA-8230 electron microprobe using *Probe for EPMA* software, operating at an accelerating voltage of 15 kV, with a beam current of 10 nA and 8 μm spot diameter. Jeankempite contains major Ca and As, with trace Na, Mg and S; no other elements were detected. Matrix effects were accounted for using the $\phi\rho(z)$ correction routine (Pouchou and Pichoir, 1991) and the analytical data are given in Table 1. The presence of H₂O and AsO₃OH groups was confirmed by infrared and Raman spectroscopy. The empirical formula has been calculated based upon 23 O from the structure and 16 H atoms per formula unit (apfu) as determined by TGA: (Ca_{4.97}Na_{0.013}Mg_{0.017})(As_{3.99}S_{0.01})₄O₂₃H₁₆. The ideal formula is Ca₅(AsO₄)₂(AsO₃OH)₂(H₂O)₇, which requires CaO 31.71, As₂O₅ 51.99, H₂O 16.30, for a total 100 wt.%.

Powder X-ray diffraction

Room temperature powder X-ray diffraction (PXRD) data (Table 2) were recorded using a Rigaku R-Axis Rapid II curved imaging plate microdiffractometer with monochromatised MoK α radiation. A Gandolfi-like motion on the ϕ and ω axes

Table 4. Atomic coordinates and equivalent isotropic displacement parameters (Å²) for jeankempite.

Atom	<i>x</i>	<i>y</i>	<i>z</i>	<i>U</i> _{eq} / <i>U</i> _{iso}
As1	0.3421(3)	0.38702(13)	0.07473(11)	0.0106(6)
As2	0.6489(3)	-0.06371(12)	0.26132(11)	0.0091(6)
As3	0.3503(3)	0.71634(12)	0.42529(11)	0.0096(6)
As4	-0.1256(3)	0.11259(13)	0.41834(11)	0.0094(6)
As5	0.1193(3)	0.54254(13)	0.24921(11)	0.0118(6)
As6	0.8551(3)	0.76914(13)	0.10389(11)	0.0106(6)
Ca1	0.1555(5)	-0.0803(3)	0.3520(2)	0.0116(12)
Ca2	0.8476(5)	0.4062(2)	-0.0162(2)	0.0101(12)
Ca3	0.8442(5)	0.7286(3)	0.3339(2)	0.0118(13)
Ca4	0.2774(5)	0.1515(2)	0.2295(2)	0.0160(13)
Ca5	0.3399(5)	0.7664(2)	0.1988(2)	0.0111(13)
Ca6	0.3485(5)	0.1114(3)	0.5151(2)	0.0131(13)
Ca7	0.6463(5)	0.5448(3)	0.1536(2)	0.0172(14)
Ca8*	0.6553(10)	0.4980(5)	0.4175(4)	0.016(3)
O1	-0.3298(15)	0.0536(7)	0.4518(6)	0.008(2)
O2	0.6527(15)	0.7070(7)	0.1357(6)	0.012(3)
O3	0.3283(15)	0.5999(7)	0.2216(6)	0.011(2)
O4	0.4112(15)	0.4798(7)	0.1004(6)	0.012(3)
O5	0.0321(15)	0.0778(7)	0.3395(6)	0.009(2)
O6	0.5466(16)	0.3256(7)	0.0360(7)	0.013(3)
O7	0.8149(15)	-0.1043(7)	0.3391(6)	0.009(2)
O8	0.5817(15)	0.1839(7)	0.5621(6)	0.009(2)
O9	0.1822(15)	0.7535(7)	0.3488(6)	0.010(2)
O10	0.8310(17)	0.7021(8)	0.4978(7)	0.019(3)
O11	0.5492(16)	0.6520(8)	0.3894(7)	0.016(3)
O12	-0.0265(17)	0.5688(8)	0.3359(7)	0.019(3)
O13	0.5760(16)	0.8373(8)	0.2474(7)	0.016(3)
O14	0.2328(16)	0.6567(7)	0.5223(6)	0.013(3)
O15	0.9922(16)	0.5523(7)	0.1637(6)	0.011(3)
O16	0.7706(16)	0.8862(8)	0.0571(7)	0.016(3)
O17	0.1851(15)	0.4345(7)	-0.0035(6)	0.010(2)
O18	0.4485(15)	0.0027(7)	0.2952(6)	0.010(2)
O19	0.2718(18)	0.4846(8)	0.4519(8)	0.028(3)
O20	0.1724(17)	-0.0685(8)	0.1919(7)	0.018(3)
O21	0.3383(16)	0.8223(8)	0.0395(7)	0.016(3)
O22	0.9979(16)	0.2558(7)	-0.0177(6)	0.015(3)
O23	0.1982(17)	0.4203(8)	0.2879(7)	0.021(3)
O24	0.9909(15)	0.7624(7)	0.1859(6)	0.009(2)
O25	0.8229(16)	0.3768(8)	0.1500(7)	0.017(3)
O26	-0.2067(15)	0.2303(7)	0.3678(6)	0.010(2)
O27	0.6152(18)	0.2096(8)	0.1923(7)	0.025(3)
O28	0.0035(15)	0.1137(8)	0.5009(6)	0.011(3)
O29	0.7750(15)	-0.0033(7)	0.1644(6)	0.010(2)
O30	0.3587(16)	0.2123(8)	0.3583(7)	0.017(3)
O31	0.4037(16)	0.0789(8)	0.1035(7)	0.018(3)
O32	-0.0054(17)	0.1446(8)	0.1451(7)	0.022(3)
O33	0.2139(16)	0.3187(8)	0.1662(7)	0.016(3)
O34*	0.617(3)	0.4358(15)	0.2983(13)	0.013(5)
O34*	0.629(4)	0.4846(18)	0.3280(15)	0.025(6)
O35**	0.345(19)	0.833(9)	-0.081(8)	0.03(3)

*0.5 occupancy, **0.1 occupancy.

was used to randomise diffraction from the sample. Observed *d* values and intensities were derived by profile fitting using *JADE 2010* software (Materials Data, Inc.). Unit-cell parameters refined from the powder data using whole pattern fitting in *JADE 2010* are as follows: *a* = 6.704(5) Å, *b* = 14.912(5) Å, *c* = 15.926(5) Å, α = 73.56(2)°, β = 81.99(2)°, γ = 82.81(2)° and *V* = 1506.0(13) Å³.

Single-crystal X-ray diffraction

Single-crystal X-ray diffraction data were collected at 150 K using an Apex II CCD-based detector and MoK α X-rays from a micro-focus source mounted to a Bruker Quazar three-circle diffractometer. Corrections for Lorentz, polarisation and background effects were made using the Bruker program *SAINT* within the *Apex3*

Table 5. Anisotropic atomic displacement parameters (\AA^2) for jeankempite.

Site	U^{11}	U^{22}	U^{33}	U^{12}	U^{13}	U^{23}
As1	0.0068(10)	0.0130(10)	0.0147(9)	-0.0023(8)	-0.0041(7)	-0.0060(8)
As2	0.0049(10)	0.0131(10)	0.0117(9)	-0.0038(8)	-0.0038(7)	-0.0048(8)
As3	0.0053(10)	0.0119(10)	0.0138(9)	-0.0019(8)	-0.0068(7)	-0.0036(8)
As4	0.0048(10)	0.0139(10)	0.0117(9)	-0.0029(8)	-0.0043(7)	-0.0046(8)
As5	0.0103(10)	0.0149(10)	0.0126(9)	-0.0017(8)	-0.0042(7)	-0.0059(8)
As6	0.0069(10)	0.0150(10)	0.0134(9)	-0.0010(8)	-0.0057(7)	-0.0074(8)
Ca1	0.0054(19)	0.015(2)	0.0151(18)	-0.0018(15)	-0.0055(14)	-0.0031(16)
Ca2	0.009(2)	0.013(2)	0.0109(17)	-0.0012(16)	-0.0039(14)	-0.0046(15)
Ca3	0.0060(19)	0.016(2)	0.0181(19)	-0.0036(15)	-0.0042(14)	-0.0096(16)
Ca4	0.0084(19)	0.018(2)	0.0215(19)	-0.0021(15)	-0.0056(15)	-0.0024(16)
Ca5	0.0033(19)	0.018(2)	0.0154(18)	-0.0016(16)	-0.0037(14)	-0.0083(16)
Ca6	0.009(2)	0.020(2)	0.0137(18)	-0.0054(17)	-0.0036(15)	-0.0077(16)
Ca7	0.005(2)	0.021(2)	0.034(2)	-0.0025(16)	-0.0060(16)	-0.0187(18)
Ca8	0.015(4)	0.018(4)	0.013(4)	0.001(3)	-0.005(3)	-0.002(3)

Table 6. Selected bond distances (in \AA) for jeankempite.

Ca1–O5	2.359(15)	Ca5–O2	2.376(18)	As1–O4	1.682(13)	Hydrogen Bonds (D...A)	
Ca1–O7	2.403(12)	Ca5–O3	2.413(12)	As1–O6	1.694(15)		O6...O33
Ca1–O8	2.482(22)	Ca5–O9	2.441(16)	As1–O17	1.687(16)	O10...O19	2.815(21)
Ca1–O9	2.475(12)	Ca5–O13	2.335(18)	As1–O33	1.713(18)	O10...O14	2.750(18)
Ca1–O18	2.387(19)	Ca5–O20	2.552(18)	<As1–O>	1.694	O10...O30	2.989(24)
Ca1–O20	2.495(12)	Ca5–O21	2.440(15)	As2–O7	1.713(15)	O16...O29	2.693(21)
Ca1–O28	2.379(19)	Ca5–O24	2.389(11)	As2–O13	1.692(14)	O16...O31	2.850(21)
<Ca1–O>	2.426	<Ca5–O>	2.421	As2–O18	1.686(15)	O19...O12	2.844(27)
Ca2–O4	2.514(23)	Ca6–O1	2.415(18)	As2–O29**	1.719(17)	O19...O34'	2.885(33)
Ca2–O6	2.407(19)	Ca6–O1	2.380(13)	<As2–O>	1.703	O20...O13	3.015(24)
Ca2–O15	2.389(18)	Ca6–O7	2.407(16)	As3–O8	1.680(12)	O20...O31	2.778(27)
Ca2–O17	2.401(13)	Ca6–O8	2.321(17)	As3–O9	1.706(15)	O20...O29	2.771(29)
Ca2–O17	2.460(12)	Ca6–O10	2.849(19)	As3–O11	1.674(16)	O21...O31	2.829(28)
Ca2–O22	2.344(16)	Ca6–O28	2.352(11)	As3–O14	1.692(16)	O21...O6	2.777(22)
Ca2–O25	2.545(13)	Ca6–O30	2.523(20)	<As3–O>	1.688	O21...O22	2.770(21)
<Ca2–O>	2.437	<Ca6–O>	2.464	As4–O1	1.664(15)	O23...O30	3.091(24)
Ca3–O7	2.497(12)	Ca7–O2	2.358(12)	As4–O5	1.681(15)	O23...O33	2.762(22)
Ca3–O9	2.398(12)	Ca7–O3	2.412(18)	As4–O28	1.678(14)	O23...O34	2.880(25)
Ca3–O10	2.520(13)	Ca7–O4	2.317(17)	As4–O26*	1.762(15)	O25...O33	2.681(18)
Ca3–O11	2.348(19)	Ca7–O15	2.368(12)	<As4–O>	1.696	O25...O27	2.876(24)
Ca3–O12	2.422(16)	Ca7–O17	2.453(16)	As5–O3	1.676(15)	O25...O34	2.868(30)
Ca3–O13	2.541(23)	Ca7–O25	2.644(18)	As5–O12	1.689(16)	O26...O30	2.990(16)
Ca3–O24	2.365(16)	Ca7–O34'	2.659(25)	As5–O15	1.669(14)	O26...O34	3.088(30)
<Ca3–O>	2.442	<Ca7–O>	2.459	As5–O23*	1.786(15)	O27...O6	2.663(24)
Ca4–O5	2.356(22)	Ca8–O11	2.251(17)	<As5–O>	1.705	O27...O32	2.691(21)
Ca4–O18	2.340(20)	Ca8–O12	2.526(22)	As6–O2	1.679(15)	O29...O31	2.806(23)
Ca4–O27	2.463(17)	Ca8–O14	2.304(19)	As6–O16**	1.747(16)	O29...O32	2.726(22)
Ca4–O30	2.612(17)	Ca8–O19	2.294(17)	As6–O24	1.669(14)	O32...O22	2.654(23)
Ca4–O31	2.539(19)	Ca8–O19	2.576(16)	<As6–O>	1.693	O34...O14	3.053(29)
Ca4–O32	2.502(18)	Ca8–O34	2.393(27)	As6–O22	1.678(15)	O34'...O14	2.876(34)
Ca4–O33	2.416(17)	<Ca8–O>	2.391	As6–O24	1.669(14)	O34'...O12	2.799(34)
<Ca4–O>	2.461					O35...O29	2.595(12)

*Acidic OH; **disordered acidic OH.

suite of programs. A multi-scan semi-empirical absorption correction was applied using equivalent reflections in *SADABS-2015* (Krause, 2015). The $|E^2-1|$ value calculated during data reduction was close to that expected for a centrosymmetric structure (~ 0.98), and an initial solution in the space group $P\bar{1}$ was given via the *Superflip* algorithm (Palatinus and Chapuis, 2007) within the *JANA2006* software package (Petříček *et al.*, 2014). The structure was refined on the basis of F^2 to a final R_1 of 0.0591 for 2781 reflections with $I_{\text{obs}} > 3\sigma I$. The final model included anisotropic-displacement parameters for atoms

except O and the data were not of sufficient quality to locate H atoms; however, hydrogen-bond strengths for select atoms are calculated on the basis of O–O interatomic distances. Further details regarding the data collection and refinement are given in Table 3. The atomic coordinates and equivalent displacement parameters are given in Table 4, anisotropic displacement parameters in Table 5 and interatomic distances in Table 6. The bond-valence sums, calculated using the parameters of Gagné and Hawthorne (2015) and hydrogen-bond strength from Ferraris and Ivaldi (1988) are presented in Table 7. The

Table 7. Bond-valence analysis in valence units* for jeankempite.

Atom	As1	As2	As3	As4	As5	As6	Ca1	Ca2	Ca3	Ca4	Ca5	Ca6	Ca7	Ca8	H bonds	Σ_{anion}	O type
O1				1.33								0.33, 0.32				1.94	O
O2						1.28					0.31		0.33			1.93	O
O3					1.29						0.29		0.29			1.87	O
O4	1.27							0.23					0.37			1.86	O
O5				1.27			0.33			0.33						1.93	O
O6	1.22							0.29							0.19, 0.25	1.96	O
O7		1.16					0.30		0.24			0.29				1.99	O
O8			1.27				0.25					0.36				1.88	O
O9			1.18				0.25		0.30		0.27					2.00	O
O10									0.22			0.10				0.32	H ₂ O
O11			1.30						0.34					0.43		2.07	O
O12					1.24				0.28					0.22	0.17	1.91	O
O13		1.23							0.21		0.35				0.13	1.92	O
O14			1.23											0.38	0.20, 0.16	1.97	O
O15					1.31			0.31						0.32		1.95	O
O16						1.05										1.05	OH
O17	1.25							0.30, 0.26					0.26			2.07	O
O18		1.23					0.31			0.35						1.91	O
O19														0.39, 0.19		0.29	H ₂ O
O20							0.24				0.21					0.44	H ₂ O
O21											0.27					0.27	H ₂ O
O22						1.28		0.34							0.20, 0.25	2.07	O
O23				0.94												0.94	OH
O24						1.31		0.33		0.31						1.95	O
O25							0.21						0.17			0.38	H ₂ O
O26				1.01												1.01	OH
O27										0.26						0.26	H ₂ O
O28				1.28			0.32					0.34				1.93	O
O29		1.14														1.14	OH
O30										0.18		0.22				0.40	H ₂ O
O31										0.21						0.21	H ₂ O
O32										0.23						0.23	H ₂ O
O33	1.17									0.29					0.24, 0.20, 0.18	2.07	O
O34														0.30		0.30	H ₂ O
O34'													0.16			0.17	H ₂ O
O35																0.00	H ₂ O
Σ_{cation}	4.91	4.78	4.98	4.89	4.78	4.92	1.99	1.94	1.92	1.85	2.02	1.92	1.90	1.92			

*Bond-valence parameters are from Gagné and Hawthorne (2015). Bond valences to select O atoms are included, while contributions to H₂O and OH sites are not. Hydrogen-bond strengths are based on O...O bond lengths from Ferraris and Ivaldi (1988). Anion sums for atom O19 are scaled to account for disorder.

crystallographic information file has been deposited with the Principal Editor of *Mineralogical Magazine* and is available as Supplementary material (see below).

Features of the crystal structure

The crystal structure of jeankempite is built from a network of edge- and vertex-sharing CaO₆, CaO₇ and AsO₄ polyhedra (Fig. 5). Atoms Ca1 through Ca7 are coordinated by seven oxygen atoms as irregular polyhedra, whose shape can be likened to an octahedron with one double vertex. Ca8 is a six-coordinated distorted octahedron disordered over the inversion centre with 0.5 occupancy and total site population of 1 Ca apfu. The Ca–O distances are close to expected values except for the Ca6–O10 distance of 2.85 Å, although similarly long Ca–O distances up to 2.87 Å are observed in guérinite (Catti and Ferraris, 1974). All As atoms occur as tetrahedral arsenate groups and several form bonds to oxygen atoms that are fully protonated (As4 and As5) or partially protonated (As2 and As6) based on bond-valence calculations and are distinguished by their elongated As–O bonds, with further details given below.

The polyhedra centred by Ca1 through Ca7 bind to edges and vertices of arsenate groups, forming a sheet parallel to {011}

which corresponds to the observed plane of perfect cleavage. Connectivity between the sheets occurs in several ways: through the interlayer atoms Ca4 and Ca8 that share O atoms of arsenate groups, by the edges shared between pairs of Ca polyhedra (Ca4–Ca1 and Ca8–Ca3) and finally through the disordered O atom of an H₂O group (O34/O34') shared between Ca8 and Ca7. The connectivity between sheets also involves significant hydrogen bonding between H₂O groups, H atoms of AsO₃OH groups and arsenate O atoms. Two empty channels, extending along {100}, occur between sheets and are rimmed by the H carriers O16, O23, O26 and O29 of the protonated arsenate groups (Fig. 6). Based on their elongated As–O bond distances (≥ 1.72 Å) and valence sums, we deduce that the first channel is lined by fully protonated atoms O23 and O26, and in the second channel by partially protonated O16 and O29, which lie only 2.69 Å apart and possibly share a disordered H atom; in total, corresponding to two OH groups pfu.

In all, 6.73 O atoms of H₂O groups were located during the refinement, and all but the isolated and partially occupied H₂O group O35 are bound to Ca atoms. The large channel formed between pairs of protonated O16, O20 and O29 atoms, measuring roughly ~ 37 Å², may accommodate an additional isolated H₂O

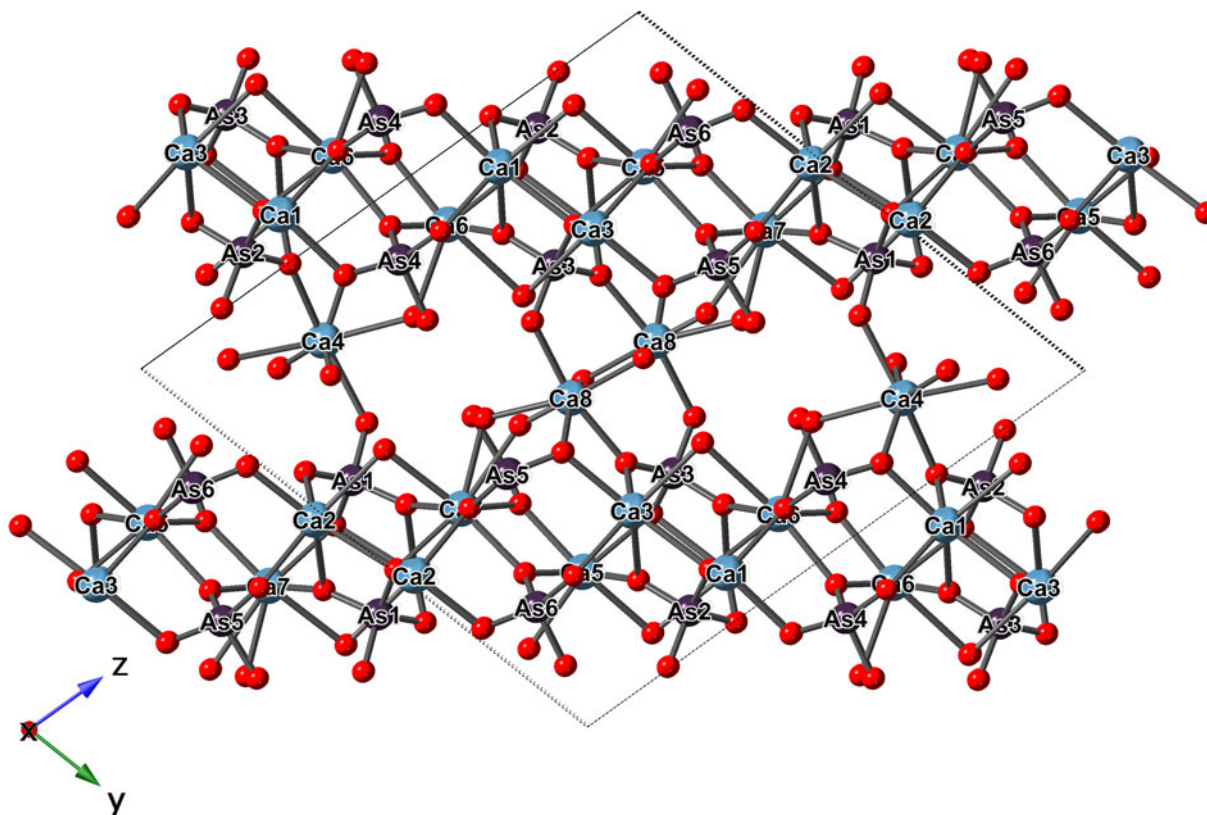


Fig. 5. The ball-and-stick representation of the structure of jeankempite.

group (i.e. \sim seven H_2O pfu), but there were no significant difference-Fourier density residues present. Based on the thermogravimetric analyses and congruence between the chemical, density and optical data, we propose the ideal formula for jeankempite as $\text{Ca}_5(\text{AsO}_4)_2(\text{AsO}_3\text{OH})_2(\text{H}_2\text{O})_7$.

Topotactic dehydration and relationship to other species

Jeankempite is related structurally to guérinite, having a z parameter two thirds that of guérinite and a more ordered structure (Fig. 7). In the structure of guérinite, $(\bar{1}01)$ layers of Ca- and As-centred polyhedra are linked by shared vertices, edges, and faces of interlayer Ca polyhedra and numerous hydrogen bonds (Catti and Ferraris, 1974). The $(\bar{1}01)$ layers are interrupted along $[001]$ by two disordered Ca atoms, distributed over 4 sites with a combined occupancy of one Ca apfu. Considering the intimate intergrowth of jeankempite and guérinite observed in PXRD analyses, we hypothesise that jeankempite may have formed through a topotactic reaction resulting from the dehydration of guérinite. In a topotactic reaction, structural rearrangements occur in the solid state along crystallographically equivalent orientations relative to the parent crystal, with an exchange of local components that proceeds throughout the entire volume of the parent crystal, resulting in the conservation of certain structural elements of the parent in one, two, or three dimensions (Günter and Oswald, 1975). The potential topotactic relationship between jeankempite and guérinite is revealed when comparing the arrangement of arsenate tetrahedra in each mineral (Fig. 8). Upon dehydration, reorganisation of hydrogen bonds and convergence of the guérinite $(\bar{1}01)$ layers may proceed approximately along $[201]$, locking into place to

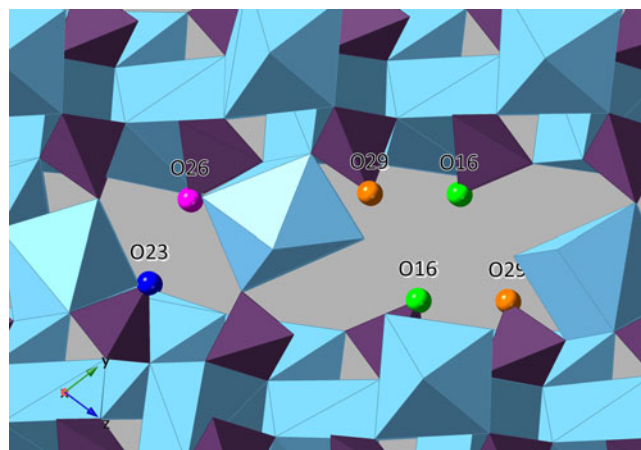


Fig. 6. A view along a of the two empty channels found within the interlayer of jeankempite.

form contiguous sheets as found in jeankempite. A layer shift from the guérinite structure would be accompanied by reordering of the two disordered Ca atoms and relocation of one interlayer Ca atom to the newly formed sheet, yielding the disordered dimeric Ca8 configuration in jeankempite. According to the scheme for topotactic reactions developed by Günter and Oswald (1975), the rearrangement can be classified as the type in which three-dimensional structural elements are conserved; in this case, sections of the disordered $(\bar{1}01)$ layers in guérinite become infinite sheets in jeankempite. Several Ca–O/Ow and As–O–Ca bonds must be broken to achieve layer convergence during dehydration, suggesting

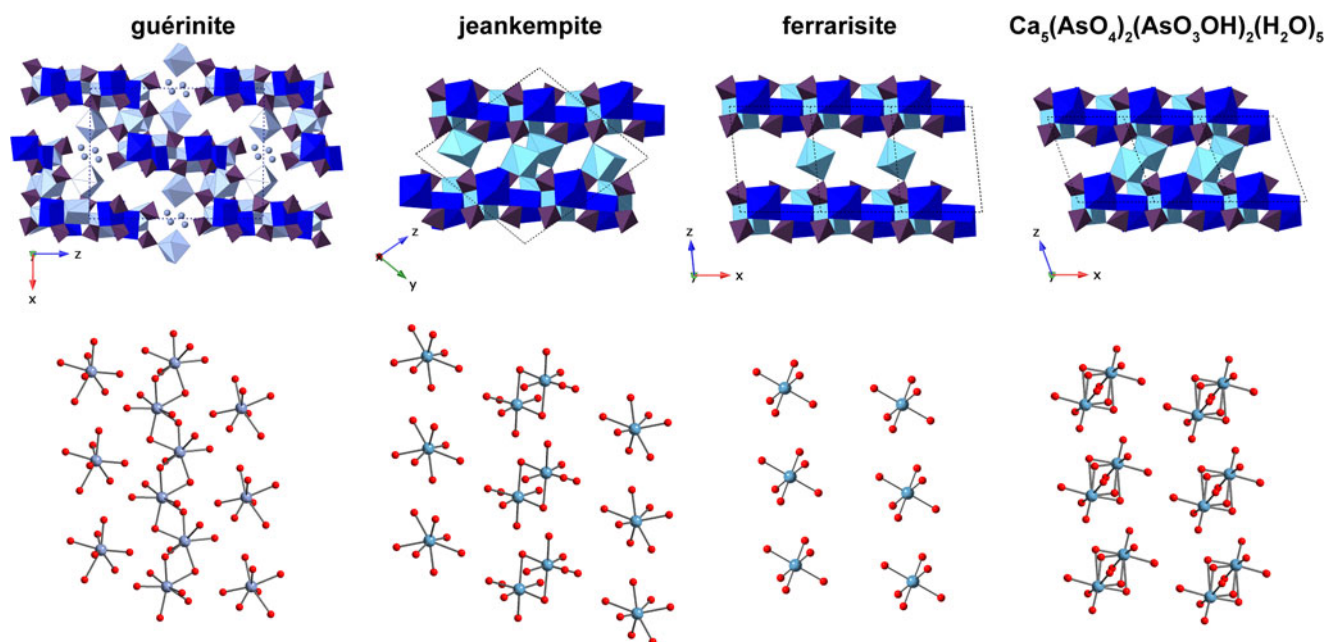


Fig. 7. A comparison of the layer (top) and interlayer (bottom) arrangement in jeankempite with related arsenates. Calcium polyhedra are presented in shades of blue and teal, arsenate tetrahedra are purple and O atoms are red spheres. Disordered calcium atoms in the polyhedral representation of guérinite are shown as light blue spheres. Some O of lattice H_2O are omitted for clarity.

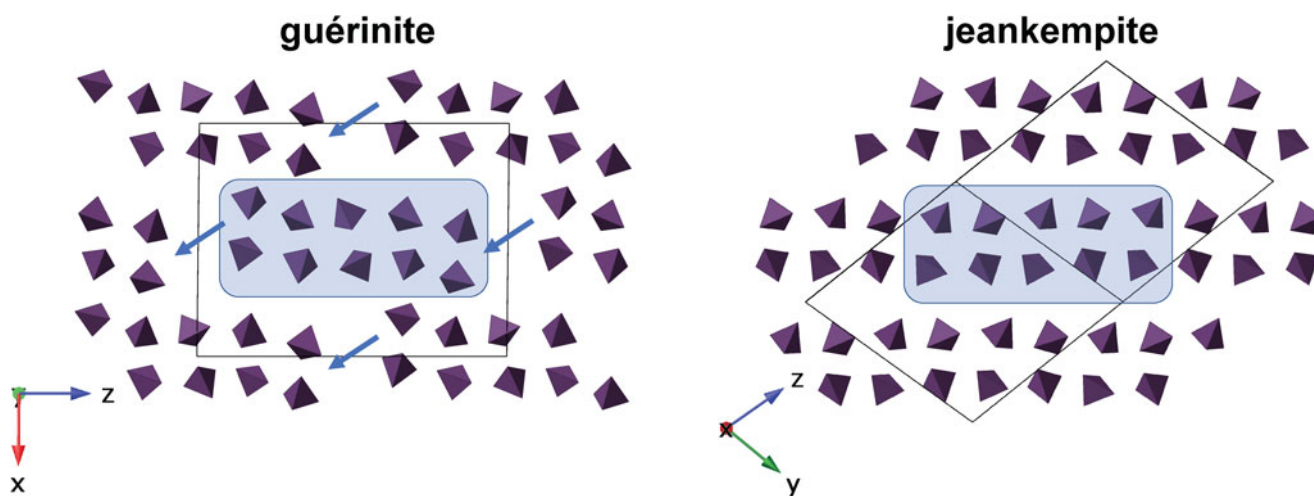


Fig. 8. Diagram depicting the possible topotactic rearrangement during dehydration from guérinite to jeankempite. Arsenate tetrahedra are shown in purple, with the unit cell as a solid black line.

that the reaction kinetics may proceed relatively slowly, because such rearrangements require higher activation energy than those involving loss of loosely bound H_2O molecules; e.g. phaunouxite $\text{Ca}_3(\text{AsO}_4)_2 \cdot 11\text{H}_2\text{O} \rightarrow$ rauenthalite $\text{Ca}_5(\text{AsO}_4)_2 \cdot 10\text{H}_2\text{O}$ (Catti and Ivaldi, 1983). A topotactic rearrangement brought on by relatively slow dehydration may explain how the large single crystals of jeankempite studied here were able to form from pre-existing guérinite.

The structure of jeankempite also closely resembles ferrarisite and the dehydrated phase $\text{Ca}_5(\text{AsO}_4)_2(\text{AsO}_3\text{OH})_2 \cdot 5\text{H}_2\text{O}$, produced by heating ferrarisite (Catti and Ivaldi, 1981) (Fig. 7). Sheets in these three structures are nearly identical, deviating only marginally with respect to the orientation of Ca- and As-centred polyhedra and the alignment of adjacent layers. Together with the pentahydrate phase, Ferraris *et al.* (1980)

observed an additional unidentified dehydration product of ferrarisite that was distinct from the first two dehydration products of guérinite. Unfortunately, structural data for the dehydration products are no longer available and will require re-examination using a combination of natural and synthetic material heated at variable rates (M. Catti, 2018, pers. comm.). Jeankempite and the unknown calcium arsenate hydrate detected on the holotype specimen may be related to the unidentified dehydration phases produced by heating, and we intend to explore these potential relationships while searching for additional evidence of topotactic reactions brought on by dehydration of calcium arsenate minerals.

Supplementary material. To view supplementary material for this article, please visit <https://doi.org/10.1180/mgm.2020.92>

Acknowledgements. We thank Dr Igor Pekov and an anonymous reviewer for valuable comments that improved the quality of this manuscript. Support for this work is provided by the Chemical Sciences, Geosciences and Biosciences Division, Office of Basic Energy Sciences, Office of Science, U.S. Department of Energy, Grant No. DE-FG02-07ER15880. We thank the ND Energy Materials Characterization Facility for use of the single-crystal X-ray diffraction instrument. DSC-TGA work was supported by funding, collaboration, services and infrastructure through the Nuclear Science Center User Facility and Alexandra Navrotsky Institute for Experimental Thermodynamics at WSU. EPMA work was performed at the Geoanalytical Laboratory at WSU. A portion of this study was funded by the John Jago Trelawney Endowment to the Mineral Sciences Department of the Natural History Museum of Los Angeles County.

References

- Amphalop N., Suwantarant N., Prueksasit T., Yachusri C. and Srithongouthai S. (2020) Ecological risk assessment of arsenic, cadmium, copper, and lead contamination in soil in e-waste separating household area, Buriram Province, Thailand. *Environmental Science and Pollution Research*, <https://doi.org/10.1007/s11356-020-10325-x>
- Asante K.A., Agusa T., Biney C.A., Agyekum W.A., Bello M., Otsuka M., Itai T., Takahashi S. and Tanabe S. (2012) Multi-trace element levels and arsenic speciation in urine of e-waste recycling workers from Agbogboshie, Accra in Ghana. *Science of The Total Environment*, **424**, 63–73.
- Bornhorst T.J., Paces J.B., Grant N.K., Obradovich J.D. and Huber N.K. (1988) Age of native copper mineralization, Keweenaw Peninsula, Michigan. *Economic Geology*, **83**, 619–625.
- Brown A.C. (2006) Genesis of native copper lodes in the Keweenaw District, Northern Michigan: A hybrid evolved meteoric and metamorphogenic model. *Economic Geology*, **101**, 1437–1444.
- Butler B.S. and Burbank W.S. (1929) The copper deposits of Michigan. pp. 238. *U.S. Geological Survey Professional Paper 144*. United State Government Printing Office, Washington, DC.
- Catti M. and Ferraris G. (1974) Crystal structure of $\text{Ca}_5(\text{HAsO}_4)_2(\text{AsO}_4)_2 \cdot 9\text{H}_2\text{O}$ (guérinite). *Acta Crystallographica*, **B30**, 1789–1794.
- Catti M. and Ivaldi G. (1981) Mechanism of the reaction $\text{Ca}_5\text{H}_2(\text{AsO}_4)_4 \cdot 9\text{H}_2\text{O}$ (ferrarisite) \rightarrow $\text{Ca}_5\text{H}_2(\text{AsO}_4)_4 \cdot 5\text{H}_2\text{O}$ and structure of the latter phase. *Zeitschrift für Kristallographie - Crystalline Materials*, **157**, 119–130.
- Catti M. and Ivaldi G. (1983) On the topotactic dehydration $\text{Ca}_3(\text{AsO}_4)_2 \cdot 11\text{H}_2\text{O}$ (phaunouxite) \rightarrow $\text{Ca}_3(\text{AsO}_4)_2 \cdot 10\text{H}_2\text{O}$ (rauenthalite), and the structures of both minerals. *Acta Crystallographica*, **B39**, 4–10.
- Cullen W.R. and Reimer K.J. (1989) Arsenic speciation in the environment. *Chemical Reviews*, **89**, 713–764.
- Dyl S.J. (2002) In memoriam: Jean Petermann Kemp Zimmer (1917–2001). *Rocks & Minerals*, **77**, 420–421.
- Ferraris G. and Ivaldi G. (1988) Bond valence vs bond length in O...O hydrogen bonds. *Acta Crystallographica Section*, **B44**, 341–344.
- Ferraris G., Chiari G. and Catti M. (1980) The structure of ferrarisite, $\text{Ca}_5(\text{HAsO}_4)_2(\text{AsO}_4)_2 \cdot 9\text{H}_2\text{O}$, disorder, hydrogen bonding and polymorphism with guérinite. *Bulletin De Minéralogie*, 541–546.
- Gagné O.C. and Hawthorne F.C. (2015) Comprehensive derivation of bond-valence parameters for ion pairs involving oxygen. *Acta Crystallographica*, **B71**, 562–578.
- Günter J.R. and Oswald H.R. (1975) Attempt to a systematic classification of topotactic reactions. *Bulletin of the Institute for Chemical Research, Kyoto University*, **53**, 249–255.
- Gunter, M.E., Weaver, R., Bandli, B.R., Bloss, F.D., Evans, S.H. and Su, S.C. (2004) Results from a McCrone spindle stage short course, a new version of EXCALIBUR, and how to build a spindle stage. *The Microscope*, **52**, 23–39.
- Han F.X., Su Y. Fau - Monts D.L., Monts D.L. Fau - Plodinec M.J., Plodinec M.J. Fau - Banin A., Banin A. Fau - Triplett G.E. and Triplett G.E. (2003) Assessment of global industrial-age anthropogenic arsenic contamination. *Naturwissenschaften*, **90**, 395–401.
- IUPAC (2005) *Nomenclature of Inorganic Chemistry – IUPAC Recommendations 2005*. International Union of Pure and Applied Chemistry (N.G. Connelly, R.M. Hartshorn, T. Damhus, A.T. Hutton, compilers). RSC Publishing, Cambridge, UK, 366 pp.
- Krause, L., Herbst-Irmer, R., Sheldrick, G.M. and Stalke, D. (2015) Comparison of silver and molybdenum microfocus X-ray sources for single-crystal structure determination. *Journal of Applied Crystallography*, **48**, 3–10.
- Libowitzky E. (1999) Correlation of O-H stretching frequencies and O-H...O hydrogen bond lengths in minerals. *Monatshfte Für Chemie*, **130**, 1047–1059.
- Majzlan J., Drahota P. and Filippi M. (2014) Parageneses and crystal chemistry of arsenic minerals. Pp. 17–184 in: *Arsenic: Environmental Geochemistry, Mineralogy, and Microbiology* (R.J. Bowell C.N. Alpers H.E. Jamieson K.D. Nordstrom and J. Majzlan, editors). Reviews in Mineralogy and Geochemistry, Vol. **79**. Mineralogical Society of America, Washington, DC.
- Makreski P., Todorov J., Makrievski V., Pejov L. and Jovanovski G. (2018) Vibrational spectra of the rare-occurring complex hydrogen arsenate minerals pharmacolite, picroparmacolite, and vladimirite: dominance of Raman over IR spectroscopy to discriminate arsenate and hydrogen arsenate units. *Journal of Raman Spectroscopy*, **49**, 747–763.
- Makreski P., Todorov J., Jovanovski G., Stojanovska M. and Petrushevski G. (2019) Depicting the dehydration and dehydroxylation processes in very rare hydrogen arsenate minerals. *Journal of Thermal Analysis and Calorimetry*, **135**, 2265–2276.
- Mandarino J.A. (2007) The Gladstone-Dale compatibility of minerals and its use in selecting mineral species for further study. *The Canadian Mineralogist*, **45**, 1307–1324.
- Moore P.B. (1962) Copper arsenides at Mohawk, Michigan. *Rocks & Minerals*, **37**, 24–26.
- Moore P.B. (1971) Copper-nickel arsenides of the Mohawk no. 2 mine, Mohawk, Keweenaw Co., Michigan. *American Mineralogist*, **56**, 1319–1331.
- Olds T.A., Kampf A.R., Dal Bo F., Burns P.C. and Guo X. (2018) Jeankempite, IMA 2018-090. CNMNC Newsletter No. 46, December 2018, page 1373; *Mineralogical Magazine*, **82**, 1369–1379.
- Palatinus L. and Chapuis G. (2007) Superflip – a computer program for the solution of crystal structures by charge flipping in arbitrary dimensions. *Journal of Applied Crystallography*, **40**, 786–790.
- Petríček V., Dušek M. and Palatinus L. (2014) Crystallographic computing system Jana2006: General features. *Zeitschrift Für Kristallographie*, **229**, 345–352.
- Pouchou J.L. and Pichoir F. (1991) Quantitative analysis of homogeneous or stratified microvolumes applying the model “PAP”. Pp. 31–75 in: *Electron Probe Quantitation* (K.F.J. Heinrich and D.E. Newbury, editors). Plenum Press, New York.
- Robinson G.W. (2004) *Mineralogy of Michigan by E.W. Heinrich. 2nd Edition*. A.E. Seaman Mineral Museum, Michigan Technological University, Houghton, MI, 252 pp.
- Smedley P.L. and Kinniburgh D.G. (2002) A review of the source, behaviour and distribution of arsenic in natural waters. *Applied Geochemistry*, **17**, 517–568.
- WHO [World Health Organization] (2001) *Environmental Health Criteria 224: Arsenic and Arsenic Compounds*. 2nd ed.. INCHEM (Internationally Peer Reviewed Chemical Safety Information), WHO International Programme on Chemical Safety, Geneva.